

**Full title:** Apyrase suppression induces major changes in the expression of genes that regulate growth and stress responses in Arabidopsis

**Authors:** Min Hui Lim<sup>a,2</sup>, Jian Wu<sup>a,2</sup>, Jianchao Yao<sup>a,2</sup>, Ignacio F. Gallardo<sup>b</sup>, Jason W. Dugger<sup>b</sup>, Lauren J. Webb<sup>b</sup>, James Huang<sup>a</sup>, Mari L. Salmi<sup>a</sup>, Jawon Song<sup>c</sup>, Greg Clark<sup>a</sup>, Stanley J. Roux<sup>a</sup>

<sup>a</sup>Department of Molecular Biosciences, The University of Texas at Austin, Austin, TX USA

<sup>b</sup>Department of Chemistry, The University of Texas at Austin, Austin, TX USA

<sup>c</sup>Texas Advanced Computing Center, The University of Texas at Austin, Austin, TX USA

<sup>1</sup>To whom correspondence should be addressed at address <sup>a</sup>

<sup>2</sup>These authors contributed equally to this work

**Running title:** Apyrase suppression induces stress-related genes

**Corresponding Author:** Stanley J. Roux  
Phone: (512) 471-4238  
Fax: (512) 232-9529  
Email: [sroux@austin.utexas.edu](mailto:sroux@austin.utexas.edu)

**ABSTRACT** Plant cells release ATP into their extracellular matrix as they grow, and extracellular ATP (eATP) can modulate the rate of cell growth in diverse tissues. Two closely related apyrases in Arabidopsis, APY1 and APY2, function in part to control the concentration of eATP. The expression of *APY1/APY2* can be inhibited by RNAi, and this suppression leads to an increase in the concentration of eATP in the extracellular medium and severely reduces growth. To clarify how the suppression of *APY1* and *APY2* is linked to growth inhibition the gene expression changes that occur in seedlings when apyrase expression is suppressed were assayed by microarray and qRT-PCR analyses. A Gene Ontology analysis revealed that the most significant gene expression changes induced by apyrase suppression were in genes involved in biotic stress responses, which include those regulating wall composition and extensibility. These expression changes predicted specific chemical changes in the walls of mutant seedlings, and two of these, wall lignification and decreased methyl ester bonds, were verified by direct analyses. Taken together the results are consistent with the hypothesis that APY1 and APY2 play an important role in the signaling steps that link biotic stresses to plant defense responses and growth changes.

**Key words:** biotic stress, lignification, pectin methylesterase, reactive oxygen species, Type III wall peroxidases

## INTRODUCTION

Plant cells release ATP into their ECM or into the growth medium when they are wounded (Song et al., 2006), and as they grow (Kim et al., 2006; Wu et al., 2007). Dose-response assays indicate that extracellular ATP (eATP) can modulate the rate of cell growth, with low concentrations promoting growth and higher concentrations inhibiting it (Clark and Roux, 2009; Roux and Steinebrunner, 2007). These data implicate a regulatory role for ectoapyrases (ecto-NTPDases) that can hydrolyze extracellular NTPs and thus limit their accumulation, and in animals ecto-NTPDases are key regulators of the concentration of extracellular ATP [eATP] (Knowles, 2011).

Two closely apyrases in Arabidopsis with high sequence similarity, APY1 and APY2, play a major role in growth regulation (Wu et al., 2007) in part because their expression is required for normal auxin transport (Liu et al., 2012). Recent evidence indicates they have a Golgi localization (Schiller et al., 2012); (Chiu et al., 2012), where they could regulate growth by controlling glycoprotein, glycolipid and wall polysaccharide synthesis. One source of eATP is secretory vesicles that have a high ATP concentration in their lumen. These secretory vesicles are derived from Golgi, therefore the activity of APY1 and APY2 in Golgi could control the luminal [ATP] in secretory vesicles and thus indirectly control the [eATP]. It is also possible that some fraction of the cellular APY1 and APY2 population function as ectoapyrases on the plasma membrane, since externally applied polyclonal antibodies that inhibit the activity of APY1 and APY2 rapidly inhibit the growth of pollen tubes, and the decrease in tube growth is accompanied by a transient increase in the [eATP] (Wu et al., 2007).

The inhibitory effects on both growth and auxin transport that result from suppressing the expression of *APY1* and *APY2* can be duplicated by raising the [eATP] (Liu et al., 2012; Tang et al., 2003). Moreover, overexpression of *APY1* or *APY2* can significantly increase the growth rate of diverse tissues (Wu et al., 2007), and this result can also be obtained by lowering the [eATP] (Clark et al., 2010b). These results, taken together, are consistent with the hypothesis that one function of APY1 and APY2 is to limit the [eATP], whether this function happens solely in Golgi or both in Golgi and on the plasma membrane.

Mutants that are null for both *APY1* and *APY2* (*apy1apy2*) are male sterile because pollen knocked out in both genes cannot germinate (Steinebrunner et al., 2003). However, the inducible suppression of *APY1* by RNAi in the background of an *apy2* knockout yields viable plants,

although these plants are dwarf (Wu et al., 2007). In the R2-4A line of mutants *APY2* is knocked out, *APY1* suppression is induced by estradiol, and the induced decrease in *APY1* transcripts occurs gradually, declining to about 30% of wild-type levels by 3.5 d, at which point growth inhibitory effects become strikingly obvious.

When applied nucleotides alter growth rates, they do so through signaling changes that include an increase in  $[Ca^{2+}]_{cyt}$  (Demidchik et al., 2003; Demidchik et al., 2011; Demidchik et al., 2009; Jeter et al., 2004; Tanaka et al., 2010b), an increase in ROS production (Demidchik et al., 2009; Song et al., 2006), and an increase in NO production (Clark et al., 2010a; Clark et al., 2010b; Reichler et al., 2009; Torres et al., 2008). As reviewed by (Clark and Roux, 2011), these signaling changes are needed for downstream changes in growth. Given that the transduction steps between early signaling changes and growth changes typically include gene expression changes, information on what genes are up- or down-regulated when the suppression of *APY1* and *APY2* leads to growth inhibition will clarify the mechanisms that link these two changes.

Suppression of apyrase expression by RNAi inhibits both the shoot and root growth of seedlings whether they are grown in light or darkness (Wu et al., 2007). To identify genes that are similarly up- or down-regulated in dark-grown and light-grown seedlings, microarray and qRT-PCR analyses of transcript changes that occurred when *APY1* and *APY2* genes are suppressed were carried out. Although apyrase suppression induces expression changes in hundreds of genes, changes in the expression of genes encoding stress-responsive and growth-regulatory wall proteins in *Arabidopsis* are especially dramatic and are highlighted in this report.

## RESULTS

### **Overview: Hundreds of Genes Change Expression When the Expression of AtAPY1 and AtAPY2 Are Suppressed.**

The suppression of *APY1* by mRNA interference (mRNAi) in plants homozygous for the *apy2* knockout mutation results in severe inhibition of root and shoot growth (Wu et al., 2007). In dark-grown RNAi lines the growth inhibition of estradiol-induced plants begins to appear at 2.5 d, but is not obvious in all plants until 3.5 d. Surprisingly, this is how long it takes to reduce *APY1* transcript levels in whole seedlings to the lowest point they reach, ~30% of that in

uninduced RNAi lines or wild-type plants (Wu et al., 2007). In dark-grown plants, the growth differences are most obvious in hypocotyls; in light-grown plants, the growth differences are most obvious in roots (Wu et al., 2007). We compared transcript abundance differences between wild-type plants and RNAi mutants grown continuously in the estradiol inducer for 3.5 d (dark grown) or for 6.0 d (light grown) using the NimbleGen Arabidopsis 4-Plex microarray, with 3 replicates. Results revealed the identity of genes whose expression significantly changed (i.e., more than 2-fold, with false discovery rate of less than 5%) after apyrase suppression.

Statistically significant changes in the transcript abundance of several hundred genes, including scores encoding wall/ECM-localized proteins, were observed, and scores of these changes were common to both dark- and light-grown mutants suppressed in apyrase expression (Supplemental Tables 1a, 1b). Control assays of wild-type plants treated with estradiol and single knock out mutants (*apy1* or *apy2*) were conducted, and only expression changes that were not induced in wild-type plants by estradiol and were not induced in single-knock out mutants are described in this report. Eighteen changes observed by microarray analysis were confirmed by qRT-PCR (Figure 1, Table 1) and RNA-Seq (data not shown).

We used qRT-PCR to determine whether the gene expression changes observed for 18 genes at 3.5 d in dark-grown plants persisted through 6.0 d, and whether the expression changes for these genes observed at 6.0 d in light-grown plants were already apparent at 3.5 d. These qRT-PCR results showed that for both light-grown and dark-grown plants most of the significant gene expression changes observed at 3.5 d were also significant at 6.0 d (Table 1).

### **Gene Ontology (GO) Category Analysis Reveals Apyrase Suppression Significantly Alters the Expression of Stress-related Genes and of Genes Encoding Proteins Expressed in the Extracellular Matrix**

Only genes that were significantly up- or down-regulated (> 2-fold; q value < 5%) were included in the GO category analyses, and they were assigned a functional categorization by annotation for GO Biological Processes. When the GO functional characterization of differentially expressed genes were divided into broad categories, the significant trends in these results showed that genes related to stress responses were the ones that most changed expression when *APY1* and *APY2* were suppressed (Supplemental Figure 1). Included among the GO Biological

processes are almost 24000 terms listed in Ontology version 1.3499. Every gene is annotated by at least one specific GO term, and most genes are annotated by more than one GO term. These more specific GO terms allow a statistical evaluation of which categories of functionally related genes changed most significantly when apyrases were suppressed (Table 2). In these Tables the “Overlap count” is the number of genes that are annotated by a particular GO term and present within the set. The “GO count” is the total number of genes annotated in the particular GO term. Only those GO terms in which the changes had an adjusted p value of less than 0.05 as sorted by Bonferroni corrected p-values, and had at least 5 genes in the Overlap count are included in the Tables.

The GO Biological processes analysis revealed that among the up-regulated genes in light-grown plants 11 different GO terms had statistically significant overlap counts, with 9 of them clearly related to genes that are up-regulated in response to biotic stress (Table 2a). Among the genes down-regulated in the light, 10 different GO terms had statistically significant overlap counts, and 3 of the top 5 categories related to metal ion transport (Table 2b), a key function found to be down-regulated in response to biotic stress in plants (Franza and Expert, 2013). Among the up-regulated genes in dark-grown plants, 8 different GO terms had statistically significant overlap counts, and two of these were related to genes that are up-regulated in response to biotic stress (Table 2c). Among the genes down-regulated in the dark, 8 different GO terms had statistically significant overlap counts and 6 of these categories related to the transport of the key nutrients, iron or nitrate (Table 2d).

### **Apypase Suppression Induces the Up-regulation of Type III Wall Peroxidases**

Five Type III wall peroxidases that are co-expressed in roots undergoing abiotic stress ([http://csbdb.mpimp-golm.mpg.de/csbdb/dbcor/ath/ath\\_tsgq.html](http://csbdb.mpimp-golm.mpg.de/csbdb/dbcor/ath/ath_tsgq.html)) are all significantly up-regulated when *APY1* and *APY2* are suppressed in R2-4A mutants, as judged by qRT-PCR (Figure 2). All are also strongly up-regulated as judged by microarray analysis, but two of them (AT5G05340 and AT5G06730) have q values higher than 5%. Because the microarray data were obtained on whole seedlings, and all 5 peroxidases are expressed mainly in roots, we tested whether the up-regulation measured in roots alone would be higher than in the whole seedlings (Figure 2). When the up-regulation observed in whole seedlings was compared to that in roots

alone by qRT-PCR, a significantly higher up-regulation in the roots was observed for At5G05340 (PER 52) and for At5G06720 (PER 53) in light-grown seedlings (Figure 2A), and for these two peroxidases plus At5G06730 (PER 54) in dark-grown seedlings (Figure 2B). In most cases the fold-change observed by the qRT-PCR assay for whole seedlings was somewhat higher than that found by microarray. The genes encoding these 5 peroxidases all share common WRKY and other promoter motifs (Supplemental Table 2). WRKY46 (AT2G46400) is significantly up-regulated in induced R2-4A mutants, both in dark-grown and light-grown plants (Supplemental Table 1a).

### **Apyprase Suppression Induces the Accumulation of Hydrogen Peroxide and Lignin in Roots**

Since microarray data revealed that cell wall peroxidases are up-regulated in R2-4A, we tested how they function in R2-4A. Type III wall peroxidases use hydrogen peroxide ( $H_2O_2$ ) substrates to induce protein cross-links and lignin formation in cell walls. As assayed by DAB (3, 3'-diaminobenzidine tetrahydrochloride) staining, the  $H_2O_2$  level is increased in R2-4A roots (Figure 3A). After germination, wild-type roots maintain the same level of  $H_2O_2$  from 2d to 6d, however R2-4A roots show increased  $H_2O_2$  levels during their 3- to 6-d period of growth. They also accumulate lignin at this time (Figure 4). Lignin is accumulated in secondary cell walls, such as in mature vascular tissue (Supplemental Figure 2). Normally lignin formation does not occur in the walls of cells in the meristematic, elongation, or early-differentiated cell zones of wild-type roots. However, R2-4A seedlings develop mature vascular tissue near their root tip (Supplemental Figure 2D), and accumulate lignin not only in vascular tissue, but also in the endodermis, cortex and epidermis (Figure 4 B, D and F).

### **Apyprase Suppression Increases Cross-Linking in Cell Walls**

The most dramatic growth change that occurs when apyrases are suppressed in light-grown R2-4A seedlings is inhibition of root growth. One way to account for the growth differences between wild-type and mutant roots would be by the degree of cross-linking of homogalacturonan (HG) present in the cell walls of the plant. A commonly reported HG cross-linking mechanism involves the formation of a borate ester that covalently links two rhamnogalacturonan-II (RG-II)

monomers found on HG (Supplemental Figure 3) (Ishii et al., 1999; O'Neill et al., 2004; Vincken et al., 2003). The ester forms at *O*-2 and *O*-3 within apiosyl residues found on side chain A of RG-II. If this cross-linking occurred when the expression of APY1 and APY2 was suppressed, the mutant root samples would therefore contain fewer methyl-ester groups and more boron. To investigate this question, we examined the chemical differences between wild-type and mutant root samples with FTIR and XPS.

Although the IR spectrum of cell walls is a complicated composition of bands from many functional groups, it was possible to identify differences between the wild-type and mutant samples through FTIR spectroscopy. Figure 5a shows the average of 13 FTIR spectra for both wild-type and R2-4A-mutant root samples, combining data from both biological and instrumental repeats. We identified 13 peaks that appeared in both wild-type and mutant spectra: 1035, 1057, 1111, 1161, 1207, 1251, 1319, 1336, 1374, 1431, 1516, 1648, and 1741 cm<sup>-1</sup>. The most noticeable differences in the spectra were the decreases in intensity of peaks at 1741 and 1251 cm<sup>-1</sup> for the mutant samples (Figure 6a, red spectrum) compared to wild-type (Figure 5a, black spectrum). These peaks correspond to carbonyl (C=O) and ether (C-O) intensities, respectively, and are associated with methyl ester groups on the polysaccharide chains (Nivens et al., 2001; Pau-Roblot et al., 2002). This decrease of methyl esters indicated that cross-linking was occurring at those sites in the cell wall, which is consistent with the mechanism for boron cross-linking proposed by Ridley *et al.* (Ridley et al., 2001). The peak at 1648 cm<sup>-1</sup> is from the amide 1 (C=O stretching) mode, and while it can be characteristic of peptide secondary structure, it does not provide any relevant information about wall cross-linking.

To determine if the decrease in intensity of the peaks at 1741 and 1251 cm<sup>-1</sup> could be used to quantitatively differentiate the wild-type and mutant samples, we used principle component analysis (PCA), a rigorous method for distinguishing wild-type and mutant samples from small differences in the complex spectra (Mouille et al., 2003). All 13 spectral peaks listed above were used in the analysis. A standard PCA analysis to calculate a covariant matrix from which the principal components (PC) were found was done with in-house scripts written in Mathematica. The clearest distinction between wild-type and R2-4A mutant samples was found when comparing the first and third principle components, shown in Figure 5b, which represented 99.3% of the observed variance between the wild-type and mutant samples. If both samples were identical in composition, the clustering of points in the PC plots would overlap; however,

the data shown in Figure 5b clearly display two distinct clusters for the wild-type (black) and mutant (red) samples, demonstrating that the small differences in infrared spectra between the wild-type and mutant samples were characteristic of the chemical composition of each sample.

Although PCA can illustrate differences between two spectra, it cannot provide a measure of their significance (Lloyd et al., 2011). To quantify these results, we integrated peaks associated with methyl ester groups involved in HG cross-linking. The averaged infrared spectrum for the mutant samples was fit using 17 Gaussian curves where peak position, intensity, and width were optimized using a Levenberg Maquardt algorithm packaged with the OPUS software. For the wild-type samples, the averaged spectrum was fit using the 17 peak positions found for the mutant samples, but peak intensity and width were optimized by the fitting routine. The Gaussian fit for the  $1741\text{ cm}^{-1}$  stretch shown in Figure 5a was found to have an actual peak position of  $1742\text{ cm}^{-1}$  after deconvolution, and the  $1251\text{ cm}^{-1}$  peak from the average spectra arose from two overlapping peaks at  $1234$  and  $1259\text{ cm}^{-1}$ . The  $1259\text{ cm}^{-1}$  peak showed no significant change between wild-type and mutant samples, whereas the  $1234\text{ cm}^{-1}$  peak accounted for the decrease in the peak intensity at  $1251\text{ cm}^{-1}$  described in Figure 5a. The peak at  $1648\text{ cm}^{-1}$  is from the amide 1 ( $\text{C=O}$  stretching) mode, and while it can be characteristic of peptide secondary structure, it does not give any relevant information about wall cross-linking bonds.

The peaks at  $1742$  and  $1234\text{ cm}^{-1}$  correspond to the  $\text{C=O}$  and  $\text{O-C-O}$  stretches of methyl ester, respectively. An example of this is shown in Figure 5c, which depicts the averaged spectra of the R2-4A mutant samples along with the Gaussian fits used to isolate the peaks associated with the methyl ester groups. This analysis indicated that the intensity of the peak at  $1742\text{ cm}^{-1}$  decreased by 21.4 % and the  $1234\text{ cm}^{-1}$  was reduced by 44.9 % compared to the WT samples. This decrease in intensity is proportional to the degree of methyl ester reduction, in agreement with the hypothesis of an increase in RG-II found on HG.

The reaction scheme in Supplemental Figure 3 proposes that bioavailable boron mediates the cross-linking of HG associated with the root cell wall. We therefore used XPS to measure the content of boron in both wild-type and mutant samples to determine if the mutants contained a greater amount of boron. The boron 1s photoelectron near 190 eV has a low cross-section of photoelectron emission (the Kratos XPS software uses a sensitivity factor of 0.159 for B 1s, compared to 0.278 for C 1s), and so to increase the sensitivity of our instrument, we opened up the detector aperture to its maximum value of 160 mm. Although this resulted in peaks with

significantly greater background noise than the C 1s and O 1s regions, we were still able to detect the B 1s peak in our samples. Representative examples of XP spectra of the B 1s peak are shown in Figure 6a, and atomic composition of both wild-type and mutant samples are given in Supplemental Table 3 (Moulder et al., 1992). Because boron is required for the normal growth of a plant, the wild-type sample contained a small amount of boron,  $0.065 \pm 0.092\%$  (Fleischer et al., 1998; O'Neill et al., 2004). However, the apyrase-suppressed mutant contained nearly 4-fold more boron ( $0.245 \pm 0.091\%$ ) than the wild-type sample. We attribute this increase in boron in the chemical composition of the cell wall to boron-mediated cross-linking of homogalacturonan.

An increase in the amount of boron mediated cross-linking in the mutant samples should also yield changes in the relative intensity of various types of carbon bonds in the cell walls. By using the 20 mm aperture, the C 1s region was also studied to understand the changes in carbon bonding. For the C 1s region, the R2-4A mutant and wild-type samples showed similar spectra with three peaks (Figure 6b). The aliphatic carbon 1s peak is shown at 285 eV and peaks at 286.6 and 287.8 eV correspond to C-(N,O) and C=O functional groups, respectively, in agreement with previously published spectra taken from cell walls (Dufrene et al., 1997; Ramstedt et al., 2011). A quantitative analysis of the C-(C,H) and C-(N,O) signal amplitudes shows that the average intensity ratio C-(N,O)/C-(C,H) is 0.744 and 0.925 for the wild-type (Figure 6b) and R2-4A mutant (Figure 6c) samples, respectively. These ratios would support an increase of 1.2-fold more C-O bonds for the R2-4A mutant. Because an increase in boron cross-linking requires an increase of C-O bonds (depicted in Supplemental Figure 2), both the B 1s and C 1s spectral measurements support an increase in boron mediated cross-linking in the R2-4A mutant.

Overall, the above FTIR and XPS results indicate there is a decrease in the presence of methyl ester groups and an increase in the concentration of boron in the R2-4A mutant. To the extent these results reflect an increase in the amount of boron mediated cross-linking between cell walls they would indirectly reflect higher methylesterase activity in the R2-4A mutant. Consistent with this conclusion, one of the pectin methylesterase (PME) inhibitor proteins that can bind PMEs and inhibit their activity, PMEI4 (At4g25250), is down-regulated in both the light (> 3.9-fold) and the dark (> 5.5-fold) in estradiol-induced R2-4A seedlings (Supplemental Table 1b). Although two PME genes were up-regulated in the dark (At5g20860 and At5g55590), two others were down-regulated either in the dark (At5g47500) or in the light (At2g45220).

### **Apypase Suppression Results in Increased [eATP] in Growth Media**

The R2-4A plants grown in liquid culture had the expected root length and root tip phenotypes previously described (Liu et al., 2012). The average length of roots on each day that [ATP] was assayed in media samples is presented (Supplemental Table 4). Estradiol-induced R2-4A plants maintained a root length of about 6 mm through the 4 d that the plants were grown in estradiol.

The experiment was performed twice, with six replicas of each sample included each time. Results were similar between these two experiments; data from one is shown in Figure 7. In both Ws wild-type and R2-4A samples the [ATP] was about 12 nM one d after transfer to liquid growth conditions with estradiol. In growth media of R2-4A plants the [ATP] was higher than that of wild-type plants starting two d after the induction of APY1 suppression. This difference steadily increased through 7-d-old seedlings (4 d after induction of RNAi), at which time the [ATP] was 31 nM. During this time the primary roots of Ws wild-type and un-induced R2-4A seedlings grew an average of 18 mm while the primary roots of R2-4A seedlings grew an average of 1.5 mm.

## **DISCUSSION**

Dark-grown 3.5-d-old seedlings are at a very different developmental stage than light-grown 6.0-d-old seedlings, yet both share the common response of significant growth inhibition in their roots and hypocotyls when the expression of APY1/APY2 is suppressed. Based on this common response we predicted that many of the genes that are similarly up- and down-regulated in the R2-4A mutants grown under these two circumstances would encode proteins especially important for growth control. Indeed many of these genes play major roles in regulating wall extensibility and/or in mediating the effects of hormones on growth. For example, on the list for genes up-regulated when *APY1* and *APY2* are suppressed (Supplemental Table 1a), two of the most up-regulated genes were Type III wall peroxidases, whose activity could inhibit growth in a number of ways, as noted below. One of the three transcription factors up-regulated on this list, NAC103, modulates the unfolded protein response to pathogen stress and inhibits growth when over-expressed in *Arabidopsis* (Sun et al., 2013). On the list for genes down-regulated when *APY1* and *APY2* are suppressed (Supplemental Table 1b), one of the most down-regulated genes is marneral synthase, recently shown to be required for growth in *Arabidopsis* (Go et al., 2012).

Two others on this list (AT4G25250-pectin methylesterase inhibitor, and AT2G33790-arabinogalactan protein 30) are among the top 10 down-regulated genes when ACC inhibits root growth (Markakis et al., 2012).

Surprisingly, however, none of the genes significantly up- or down-regulated were members of the PIN, ABCB or AUX/LAX family of auxin transport facilitators (Peer et al., 2011) (Supplemental Table 5), even though the suppression of *APY1* and 2 strongly inhibited auxin transport (Liu et al., 2012). These results point to the likelihood that the rapid growth changes induced by apyrase suppression, which are observed in less than 15 min in pollen tubes, are mediated initially by post-transcriptional changes in these transporters. Although our assays of gene expression changes in R2-4A mutants were carried out within hours after the level of *APY1* transcripts dropped to their low point after their RNAi-mediated suppression, these transcriptomic changes are surely downstream of earlier signaling changes induced by apyrase suppression.

The significant root growth inhibition and root morphology changes observed in the primary roots of seedlings suppressed in *AtAPY1* and *AtAPY2* expression (Wu et al., 2007) are reminiscent of the growth inhibition effects observed in seedlings responding to biotic and abiotic stresses, some of which appear to be mediated by ethylene and ACC (Tsang et al., 2011). Many different stresses can induce similar responses in plants, the so-called stress-induced morphogenic responses (SIMRs) (Potters et al., 2009). Examples of different stresses that induce these SIMRs in roots are exposure to heavy metals, phosphate-, iron- and sulfate deficiency, flooding, and salinity. Many studies have shown that the SIMRs in roots involve common physiological processes such as altered ROS production, hormone transport changes, inhibition of elongation and consequent formation of root hairs near the apex, and blocked cell division in the primary meristem (Potters et al., 2007). All of these changes have been documented in the roots of estradiol-induced R2-4A seedlings (Wu et al. 2007; Liu et al., 2012), so it is not surprising that the gene expression changes in these mutants would be characteristic of plants subjected to stress conditions.

Abundant documentation indicates that plants under pathogen or herbivore attack reallocate resources from growth promotion to the synthesis of defense compounds (Walters and Heil, 2007; Kempel et al., 2011). Plant responses to pathogens also typically include wall reinforcement and other changes that reduce wall extensibility (Sasidharan et al., 2011; Wolf et

al., 2012). The striking finding in our GO analyses is that although the R2-4A seedlings were grown under sterile conditions, their gene expression changes in response to apyrase suppression remarkably resembled the transcriptomic changes plants undergo when under biotic attack.

One possible explanation for this is that both biotic stress and suppression of APY1/APY2 expression release ATP into the ECM. There are reports documenting ATP release from wound sites (Song et al., 2006), and from cells stimulated by elicitors (Kim et al., 2006; Wu et al., 2008). This paper and Wu et al. (Wu et al., 2007) document that blocking apyrase expression by RNAi or by antibodies results in an increase in the [eATP]. To the extent that the release of ATP into the ECM is a signal indicating to plants that they are undergoing a biotic attack, it would not be surprising that the increased [eATP] resulting from apyrase suppression in R2-4A mutants would induce gene expression changes characteristic of those that happen when plants experience pathogen or other biotic stresses.

The increased [eATP] resulting from apyrase activity inhibition can occur within minutes (Wu et al., 2007), and the release of ATP from wounded cells or cells rendered leaky by pathogen attack would also be expected to occur within minutes. The signaling changes induced by eATP, which include increased  $[Ca^{2+}]_{cyt}$ , increased NO and ROS production, and increased MAP kinase expression (Clark and Roux, 2011; Tanaka et al., 2010a), are also induced by pathogen stress, further supporting a functional connection between increased eATP and the induction of biotic stress responses. In this regard the data of Chivasa et al., which show a significant [eATP] drop 5 or more h after salicylic acid or elicitor treatment, may indicate that a decrease in [eATP] can be a later consequence of biotic stress in plants (Chivasa et al., 2009).

Another remarkable set of related gene expression changes that we observed in *APY*-suppressed seedlings was the more than 2-fold down-regulation of 8 key genes involved plant iron acquisition. These included genes encoding IRT1, IRT2, subtilase 5BT4.12, and 5 bHLH transcription factors that turn on genes for iron transport, bHLHs 29 (=FIT1), 38, 39, 100 and 101(Kobayashi and Nishizawa, 2012). Some of these genes also encode proteins needed for phosphate, nitrate, and zinc acquisition. One obvious implication of these results is that *APY* expression is needed for normal acquisition of iron and other critical nutrients. These results may be related to the frequently-used strategy of plants under pathogen attack to decrease iron availability to pathogens, and thus would be consistent with the eATP-biotic stress connection discussed above.

Although one might expect that the signaling pathways linking different hormone treatments to growth changes would converge on similar gene expression changes, Nemhauser *et al.* (Nemhauser et al., 2006) found this is not the case. They analyzed publicly available microarray data on 7-d-old light-grown *Arabidopsis* seedlings and found that the transcript abundance changes induced respectively by ABA, auxin, brassinosteroid, cytokinin, ethylene, gibberellin, and jasmonates were remarkably dissimilar from each other. They concluded that different hormones regulate growth and other responses in plants by distinctly different networks of genes. This result suggests that the transcriptional changes that link apyrase suppression to growth inhibition could also be distinct from the transcriptional changes that occur in response to growth-inhibitory levels of any one of the hormones. Using statistical techniques similar to Nemhauser *et al.*, we found that the overall pattern of gene expression changes induced by apyrase suppression is different from patterns observed when auxin, ethylene, ABA, or brassinosteroids inhibit growth (data not shown).

Superoxide ( $O_2^-$ ) is rapidly converted to  $H_2O_2$  in cells, and peroxidases use  $H_2O_2$  as a substrate to catalyze diverse products that affect root growth (Dunand et al., 2007; Gapper and Dolan, 2006; Nakagami et al., 2006; Tsukagoshi, 2012; Tsukagoshi et al., 2010). Because the inhibition of primary root growth and up-regulation of several Type III wall peroxidases occur together in roots of estradiol-induced R2-4A mutants, we assayed ROS levels in these roots. With estradiol treatment the balance of  $O_2^-$  and  $H_2O_2$  levels in the R2-4A primary root starts to be changed near when apyrase suppression peaks (~ 3 d), and by 6 d, the level of  $H_2O_2$  is much higher than that of  $O_2^-$  (Figure 3). Maintenance of  $O_2^-$  levels is important for normal cell growth (Dunand et al., 2006; Gapper and Dolan, 2006), and when root  $H_2O_2$  levels are increased, the progression of meristematic cells through S-phase and M-phase is decreased (Tsukagoshi et al. 2012).

Along with increased  $H_2O_2$  in roots, there is an increased abundance of transcripts encoding Type III peroxidases (Figure 2 and Table 1) that can catalyze a broad range of physiological processes like crosslinking of phenolic compounds to proteins and polysaccharides, and lignin deposition (Almagro et al., 2009; Djebali et al., 2011; Passardi et al., 2005; Passardi et al., 2004; Zhang et al., 2012). Peroxidase genes are up-regulated by plants in response to biotic stresses, and their expression is associated with increased resistance to insect herbivores and pathogens (Suzuki et al., 2012). Five of the genes most up-regulated when *APY1* and 2 are

suppressed encode Type III wall peroxidases that are co-expressed in roots and up-regulated together by abiotic stresses known to inhibit root growth. The up-regulation of peroxidases is often correlated with growth inhibition through peroxidase-catalyzed wall cross-linking reactions, lignin formation, and/or the ROS changes induced by these enzymes (Pedreira et al., 2011). We have confirmed that the apyrase-suppressed mutants have much more extensive lignin formation than wild-type plants, and this difference continues to increase with time (Figures 4 B, D and F).

Among genes encoding extracellular proteins, those encoding peroxidases undergo the largest changes in transcript abundance when *APY1* and *APY2* are suppressed in R2-4A mutants. However, there are scores of other genes for extracellular proteins that undergo significant changes, so many, in fact, that these are significantly overrepresented in the GO terms for cellular components. Supplementary Table 6 lists 21 genes encoding proteins that function in the extracellular region and are up-regulated in apyrase-suppressed plants grown in the light, and it lists 48 genes that are down-regulated in these plants. An unexpected entry on the list of wall-associated genes that are significantly up-regulated in both dark-grown and light-grown plants suppressed in apyrase expression is an expansin-like B-1 protein. Expansins typically promote growth, but these plants have greatly reduced shoot and root growth. Expansin-like B proteins were identified based on sequence similarity to  $\alpha$ - and  $\beta$ -expansins, but they have not yet been experimentally demonstrated to induce cell-wall loosening. Additionally, the HFD motif conserved in the catalytic site of domain 1 of expansins is not conserved in the expansin-like B-1 protein, which might indicate it functions differently than  $\alpha$ - and  $\beta$ -expansins (Sampedro and Cosgrove, 2005).

Paralleling these wall changes are two other wall changes documented by FTIR and XPS data. These assays reveal decreased pectin methyl ester bonds, which can result in increased  $\text{Ca}^{2+}$  cross linking of wall pectins (Palin and Geitmann, 2012), and increased boron accumulation, which can inhibit root growth (Aquea et al., 2012; Reid et al., 2004). These results support the conclusion that there is a higher pectin methylesterase activity in these roots. This could result both from increased expression of some PMEs such as At5g20860 and At5g55590, which are both up-regulated in induced R2-4A seedlings grown in darkness, and from the decreased expression of PMEI, also observed in induced R2-4A mutants. The decrease by 21.4 % and 44.9 % of the 1740 and 1250  $\text{cm}^{-1}$  FTIR peaks, respectively, indicates that methyl esters have decreased proportionally; nevertheless these magnitudes are larger than the relative increase (3.8

fold) in boron signal seen by the XPS and larger than the 1.2-fold increase of C-O signal. This means that the boron mediated cross-linking does not account for all of the methyl ester loss expected to occur in the cell wall, and indicates that boron mediated cross-linking is just one of multiple pathways in which the cell wall cross-links. There are more than 20 different linkages inside the cell wall (Jolie et al., 2010). Other cross-linking mechanisms that do not use boron were not investigated and should be taken into consideration for a more quantitative analysis that would more completely account for the decrease in methyl ester groups.

Taken together, increased H<sub>2</sub>O<sub>2</sub> level, increased expression of wall peroxidases, increased lignin and boron accumulation in cell walls, and decreased pectin methyl ester bonds would all contribute to root growth inhibition by gradually decreasing the number and size of cells in meristematic and elongation zones. These changes, then, are likely transduction changes that help link apyrase suppression to the strong inhibition of growth seen in the estradiol-induced R2-4A mutants.

The suppression of APY1 and 2 results in a strong inhibition of polar auxin transport in shoots and roots (Liu et al., 2012). Wall peroxidases can catalyze the oxidative degradation of auxin (Gazarian et al., 1998; Krylov and Dunford, 1996; Potters et al., 2009), and, by promoting increased lignification of cell walls in the Caspary strip they could alter auxin transport which passes through this region as it cycles between shootward and rootward transport in primary roots (Naseer et al., 2012). It seems likely, however, that these wall changes are kinetically downstream of the NO and ROS changes that take place in less than 30 min when they are induced by increased [eATP] (Salmi et al., 2013). As noted by Liu et al. (2012), all the growth and morphology changes induced by the suppression of APY1 and 2 cannot be mimicked by increasing the [eATP]. Additional research would be needed to determine how many of the gene expression changes induced by the suppression of *APY1* and *APY2* in R2-4A seedlings are attributable to changes induced by the functions of these apyrases (e.g., Golgi functions) that are not related to signaling changes induced by increased [eATP].

## METHODS

### Plant Materials and Growth Conditions

Plant materials used in microarrays were *Arabidopsis thaliana* ecotypes Wassilewskija (Ws) and RNAi mutant line R2-4A. The RNAi construct, generation of the R2-4A line and growth conditions of the seedlings were as previously described (Wu et al., 2007). For estradiol treatment, estradiol was added into MS medium to reach a final concentration of 4 µM. Plates were placed upright in a culture chamber and grown at 23° C under 24-h fluorescent light after 3 d vernalization at 4°C. Light-grown seedlings were collected at day six. For dark-grown, plates were wrapped in aluminum foil and placed in the same growth chamber. Dark-grown seedlings were harvested at 3.5 d.

### **Total RNA Isolation and NimbleGen Microarray Experiments**

In RNAi lines we observed short hypocotyl and decreased root growth in 3.5-d-old dark grown seedlings and dramatically reduced root length in 6-d-old light grown seedlings (Wu et al., 2007). Thus we examined the gene expression changes using microarrays in these two conditions. Each microarray had 4 different treatments including RNAi mutant (DKO), *apy2* single knockout with a non-induced RNAi construct (SKO), wild type treated with estradiol (WT-E), and wild type only (WT). Three repeats were carried out in each microarray. The effects of estradiol treatment were also analyzed in both microarrays and the comparison between WT-E and WT showed low gene expression changes in the whole gene expression profile (data not shown).

*Arabidopsis* seedlings were collected and frozen in liquid nitrogen. Plant tissues were ground to fine powder with a chilled mortar and pestle. Total RNA was isolated using Spectrum™ Plant Total RNA Kit (Sigma) according to the manufacturer's instruction. Four different samples were used in each microarray experiment, one for each of the four different treatments note above, and three replicates were prepared from each of the samples. Total RNA was sent to NimbleGen and hybridized to *Arabidopsis thaliana* 4-plex arrays (Catalog no: A4511001-00-01). cDNA synthesis, sample labeling, array hybridization, scanning, data extraction, and preliminary data analysis were performed at NimbleGen.

### **Quantitative RT-PCR**

Six-day-old light grown and 3.5-day-old dark grown seedlings were used. Total RNA was extracted using Spectrum™ Plant Total RNA Kit (Sigma) according to the manufacturer's instruction. After treated with DNase I (Invitrogen), total RNA (1 $\mu$ g) was reversely transcribed to cDNA using SuperScript II Reverse Transcriptase Kit (Invitrogen). cDNA was amplified in real-time PCR reactions using SYBR Green PCR Master Mix (Applied Biosystems) with gene-specific primers (see supplement material). Real-time PCR was carried out in triplicate on each sample using an ABI 7900HT Fast Real-Time PCR System (Applied Biosystems). The relative expressions of genes were normalized to the level of a reference gene--protein phosphatase 2A (PP2A). The changes of transcripts were calculated using  $2^{-\Delta\Delta CT}$  method (Shi and Chiang, 2005).

### **Significance Analysis of Microarrays**

To determine the transcriptomic changes caused by estradiol treatment of R2-4A seedlings in each set of microarray data, the comparison between the mutant and wild-type plants treated with estradiol was conducted. Those minor changes due only to estradiol treatment of wild-type plants and due only to the single knock out (*apy2*) background were excluded. Significance Analysis of Microarrays (SAM) (Tusher et al., 2001) was used to find statistically significant genes in our microarray experiment. It considers the relative change of each gene expression level with respect to the standard deviation of repeated measurements and then assigns a score to each gene. This analysis uses a non-parametric test and a permutation idea to estimate the percentage of genes identified by chance (the false discovery rate). It does not require the assumptions of equal variances or independence of genes. SAM is run as an Excel add-in and available for download online at <http://www-stat.stanford.edu/~tibs/SAM/>.

### **Histochemistry**

Wild-type and R2-4A were grown vertically for 6 d in continuous light. For comparison of H<sub>2</sub>O<sub>2</sub> and superoxide level in roots, DAB (3, 3'-diaminobenzidine tetrahydrochloride, SIGMA D3939) and NBT (nitroblue tetrazolium, SIGMA N5514) were used respectively. Lignin staining was performed using phloroglucinol (SIGMA P3502) in ethanol and HCl. For cross section, 6-d-old

seedlings were fixed with 4% paraformaldehyde in PBS overnight, and embedded in LR White (EMS #14381). After sectioning, the specimens were stained with phloroglucinol.

The method used to observe autofluorescence of lignin, clearing root and visualization was that of (Hosmani et al., 2013), and 6-d-old seedlings were assayed. After the clearing steps, seedlings were immersed in 25% glycerol and mounted on glass slides with 50% glycerol. Autofluorescence of lignin was observed with excitation 488nm (Leica DM IRE2 confocal microscope).

## Cell Wall Isolation

Ws wild-type and R2-4A seedlings were grown on vertical plates in continuous light for 6 d. Cell wall alcohol insoluble residues were prepared with a modified online protocol (<http://cellwall.genomics.purdue.edu/techniques/7.html>). Briefly, roots of 6-d-old light-grown seedlings were harvested and immediately ground into fine powder in liquid nitrogen with a mortar and pestle. The powder was treated for 5 min at 70 °C with 50 mM Tris-HCl, pH 7.0, containing 1% SDS. Following centrifugation, the pellet was washed with water, collected on a nylon mesh filter, ball-milled (Retsch) for 10 min and then boiled in 95% ethanol for 5 min. The samples were filtered through the nylon mesh, and successively washed twice with water (70 °C) and 50% ethanol (70 °C), then washed with 70% ethanol (room temperature) and dried using a speed-vac.

## Fourier-Transform Infrared Spectroscopy (FTIR)

Cell wall powder was investigated by FTIR in potassium bromide pellets. Potassium bromide (KBr, spectroscopic grade, Thermo Electron Scientific) powder was baked overnight at 150°C under an atmosphere of N<sub>2</sub>(g) to remove water. A mixture containing the 1% (w/w) isolated cell wall powder in dry KBr was pressed into pellets approximately 1 cm in diameter and 0.5 mm thick for measurement. Vibrational spectra were obtained on a Bruker Vertex 70 Fourier transform infrared (FTIR) spectrometer in a typical absorption/transmission configuration with pellet samples mounted perpendicular to the IR beam. Before each measurement the sample

compartment was purged with dry N<sub>2</sub>(g) for 10 min. A mercury cadmium telluride (MCT) detector was used to collect 100 scans at a resolution of 4 cm<sup>-1</sup> from 500 to 4000 cm<sup>-1</sup>. Repeat spectra were collected on single pellets by translating the sample vertically in the IR beam. A total of three different preparations of cell walls (biological repeats) were measured and a total of four measurements per pellet were taken (instrumental repeats) for a total of 13 individual spectra for both WT and mutant samples. These spectra were normalized with respect to the highest intensity peak at ~1056 cm<sup>-1</sup>, and an average spectrum was determined for both the wild-type and mutant samples. These spectra were then baseline corrected with a rubber band algorithm. For quantification of IR peaks, these averaged and baseline corrected spectra were each fit to 17 Gaussian curves, which were then integrated. All spectrum manipulations were performed with the instrument software package OPUS (Bruker Optics, Inc.).

### X-ray Photoelectron Spectroscopy (XPS)

X-ray phototelectron spectroscopy was used to measure chemical differences between the composition of the powdered WT and mutant samples. A densely packed layer of powders of each sample was placed on XPS sample holder with copper tape and introduced to the XPS sample chamber. A Kratos Azis Ultra XPS with a monochromatic Al K $\alpha$  source and maintained at a pressure below  $2 \times 10^{-9}$  Torr was used to collect binding energy measurements from 0-1200 eV at a resolution of 1 eV with an illumination spot approximately 300  $\mu\text{m} \times 700 \mu\text{m}$  in dimension. Ejected photoelectrons were collected in a hemispherical electron energy analyzer that was positioned normal to the sample surface. Spectra of the C 1s and O 1s were collected for 3000 ms with the detector aperture set to 20 mm. Because of the low abundance and low cross section of photoelectron emission, photoelectrons from the B 1s orbital were collected for 300 ms with the detector aperture set to 160 mm. Although this decreased the detector resolution, it provided a high enough count rate for detection of B 1s photoelectrons. Spectra of the C 1s and O 1s regions are shown under small aperture conditions; however, quantification of the chemical composition of the sample for all elements studied is reported under large aperture conditions for consistency. A charge neutralizer was used for all measurements, and all peak positions are reported with respect to the C 1s peak at 285 eV.

All peaks were fit to a Shirley baseline, and the integrated area ( $I_x$ ) of the photoelectron peaks of interest were calculated using the Kratos XPS software. The areas of these peaks were then scaled by a sensitivity factor,  $S_x$ , of 0.278, 0.780, and 0.159, for C 1s, O 1s, and B 1s peaks, respectively. The atomic fraction of each species,  $C_x$ , was then calculated using equation 1:

$$C_x = \frac{I_x/S_x}{\sum_i I_i/S_i} \quad (1)$$

The atomic fraction was then multiplied by 100 to obtain the percent composition of each element.

To determine whether there were any changes in the type of bonds carbon was making in the cell walls, high-resolution spectra of the C 1s region were collected with the aperture set to 2 mm. These spectra were baseline corrected and fit to Gaussian functions as previously described using the OPUS software package. Individual contributions to the deconvoluted spectra were integrated to calculate the relative abundance of C-(C,H), C-(N,O), and C=O bonds.

### **Assay of [eATP] in Growth Media of Apyrase-Suppressed Seedlings**

Plant lines used in these experiments were ecotype Ws wild type and the R2-4A line described by Liu et al. (2012), in which estradiol induces suppression of APY1 in an *apy2* knockout background. Seeds were surface sterilized then allowed to soak in water at 4°C for 3 d to vernalize. Seeds were planted on standard MS media with 1% sucrose and 1% agar, then 3-d-old seedlings were transferred to liquid culture in six-well plates, which had 3 mL per well of MS media with 1% sucrose. Each plant line was grown in 4 µM estradiol prepared in DMSO to induce suppression of *APY1*, and control media with an equal volume of DMSO only. Each six-well plate contained six biological replicas of the same plant line and treatment, and the treatments were: wild type and R2-4A in DMSO only, wild type and R2-4A in 4 µM estradiol. One six-well plate was prepared for each of the days after planting that media samples were collected. The number of seedlings per well was counted and recorded after media collection.

After transfer to liquid culture, seedlings were grown for the indicated number of days with constant shaking and constant light at 22-25°C. Two h before media collection the plates were removed from the shaker and kept still. Three individual samples of 50 µL of media were removed from each well and flash frozen in liquid nitrogen. Samples were stored in -40°C until

ATP measurements were made. After media collection pictures were taken of several seedlings per treatment in order to measure root length and verify expected phenotypes (Supplemental Table 3).

The [ATP] in the growth media was determined using the ENLITEN® ATP Assay System from Promega (Sunnyvale, CA). Reactions were carried out on 96-well plates and luminescence was detected using the Mithras LB940 microplate reader (Berthold Technologies). Media samples were thawed, placed on the plate quickly and kept on ice for  $\leq$  30 min before ENLITEN® reagent was added. In each reaction, 40  $\mu$ L of ENLITEN® reagent was added to 10  $\mu$ L of media sample. An ATP standard curve from  $10^{-7}$  to  $10^{-12}$  M was included on each plate. Lumen measurements were evaluated by the Dixon's Q test for outliers. In all cases at least 4 replica samples were included in averages.

### **Accession Numbers**

Sequence data from this article can be found in the EMBL/GenBank data libraries under accession number(s) provided in the Figures and Tables.

### *FUNDING*

This work was supported by the National Science Foundation (IOS 0718890 and 1027514 to S.J.R. and G.C.). I.F.G. and J.W. D. acknowledge the Army Research Office (Grant W911NF-10-1-0280) for funding. L.J.W. holds a Career Award at the Scientific Interface from the Burroughs Wellcome Fund and is an Alfred P. Sloan Foundation Research Fellow.

### *ACKNOWLEDGMENTS*

We thank the Texas Advanced Computing Center for the use of their resources.

## FIGURE LEGENDS

**Figure 1.** Correlation Analyses between Real-Time qRT-PCR and Microarray Results.

Quantitative real-time qRT-PCR was used to validate the two microarray data sets. (A) Result of standard linear regression analysis between the fold changes observed in apyrase-suppressed light-grown plants by real-time qRT-PCR (X axis) and microarray analyses (Y axis). (B) Result of standard linear regression analysis between the fold changes observed in apyrase-suppressed dark-grown plants by real-time qRT-PCR (X axis) and microarray data (Y axis). The calculated equation and correlation value ( $R^2$ ) are shown along with the regression line.

**Figure 2.** Transcript Abundance of Five Genes Encoding Type III Wall Peroxidases in Whole Seedlings and Roots Increases in R2-4A Mutants Suppressed in Their Expression of *APY1* and *APY2*. (A) qRT-PCR results of the transcript abundance changes of 5 peroxidase genes in light-grown 6-d-old seedlings. (B) qRT-PCR results of the transcript abundance changes of 5 peroxidase genes in dark-grown 3.5-d-old seedlings. Fold changes for each gene in microarray analysis is also presented in each graph. Error bars represent standard deviation. At least three biological repeats were performed for this experiment.

**Figure 3.** Higher ROS levels Are Induced R2-4A Roots When *APY1* and *APY2* Are Suppressed. (A) Hydrogen peroxide levels in wild-type (WT) and R2-4A roots from 2 d to 6 d after estradiol treatment. DAB (3, 3'-diaminobenzidine tetrahydrochloride) was used to stain hydrogen peroxide. (B) Superoxide levels in WT and R2-4A roots from 2 d to 6 d. NBT (nitroblue tetrazolium) was used to stain superoxide. Images are representative of at least three biological repeats. Scale bar = 100  $\mu\text{m}$ .

**Figure 4.** Higher Lignin Levels Are Induced in R2-4A Roots When *APY1* and *APY2* Are Suppressed. Lignin staining of 6-d-old roots with phloroglucinol in (A) wild-type (WT) and (B) R2-4A roots. Magenta color indicates lignin. Cross sections of (C) WT and (D) R2-4A roots stained with phloroglucinol. Cross sections are from region 200~600  $\mu\text{m}$  from root tip where vascular tissue is not fully matured in WT. Lignin auto-fluorescence of WT (E) and R2-4A (F). Images are representative of at least three biological repeats. Scale bar = 100  $\mu\text{m}$  in (A) and (B), 10  $\mu\text{m}$  in (C) and (D), and 50  $\mu\text{m}$  in (E) and (F).

**Figure 5.** Cell Walls of Arabidopsis Isolated from R2-4A Mutants Suppressed in Their Expression of *APY1* and *APY2* Have Altered FTIR Spectra Indicating Fewer Methyl Ester Linkages. (A) Averaged FTIR spectra for wild-type (black) and R2-4A mutant (red) samples. The average signal was computed using 13 spectra for the mutant and 13 for the wild-type samples. Each of the spectra were obtained from 100 scans at a resolution of  $4\text{ cm}^{-1}$ . The averaged spectra were normalized to the maximum intensity peak at  $1056\text{ cm}^{-1}$  peak then baseline corrected. Dashed lines are added to highlight differences in the two spectra at  $1251$  and  $1741\text{ cm}^{-1}$ . (B) Principal component analysis (PCA) of wild-type (black squares) and mutant (red circles) samples. PC1 is plotted against PC3, accounting for 99.3% of the variance. Each point on the figure represents one of the 13 peaks selected for analysis ( $1035, 1057, 1111, 1161, 1207, 1251, 1319, 1336, 1374, 1431, 1516, 1648$ , and  $1741\text{ cm}^{-1}$ ). (C) An average spectrum of the 4A mutant samples (black) is shown here with 17 fitted Gaussian curves along with the total Gaussian fit (red). The Gaussian fits associated with stretches arising from methyl-ester groups are highlighted in green, ( $1742\text{ cm}^{-1}$ ) and blue ( $1234\text{ cm}^{-1}$ ), which correspond to C=O and O-C-O vibrations, respectively.

**Figure 6.** Cell Walls of Arabidopsis Isolated from R2-4A Mutants Suppressed in Their Expression of *APY1* and *APY2* Have Altered XP Spectra Indicating More Boron Linkages. (A) XP spectra of the B 1s region showing a peak near 190 eV for wild-type (black) and mutant (red) samples. Scans were taken at a resolution of 0.1 eV, 300 ms dwell time, and a detector aperture of 160 mm. The carbon 1s region of XP spectra of (B) wild-type and (C) R2-4A-mutant cell walls taken at a resolution of 0.1 eV, dwell time of 3000 ms, and a detector aperture of 20 mm. Spectral decomposition was done by fitting the peaks to Gaussian curves. The baseline corrected data is shown in red, Gaussian fit in blue, and peak composites as dashed lines. The aliphatic carbon (C-(C,H)) peak was adjusted to 285 eV to account for binding energy shifts due to the use of a charge neutralizer. Peaks at 286.6 and 287.8 eV correspond to C-(N,O) and C=O functional groups, respectively. When measured with respect to the 285 eV signal, the R2-4A mutant sample shows a 20% increase in the 286.6 eV peak over the wild-type.

**Figure 7.** Media [eATP] Rises with Increased Suppression of Apyrase Expression in R2-4A Seedlings. (A) Time course of increase of [ATP] in seedling growth media, based on luciferase assay luminescence in comparison to ATP standard curve. Error bars represent standard deviation, and asterisks indicate statistical significance based on p value >0.05 in a Student's t-test (B) Time course of loss of *APY1* transcripts during continuous treatment of R2-4A mutants with estradiol inducer of RNAi construct.

Genes	Dark		Light	
	3.5d	6d	3.5d	6d
AT1G07160 PP2c phosphatase	0.89 (0.42)	0.59	1.2	0.62 (0.41)
AT1G21250 cell wall-associated kinase (WAK1)	6.56 (2.01)	1.02	3.16	1.52 (4.22)
AT1G73330 protease inhibitor	0.38 (0.50)	0.51	0.78	0.38 (0.25)
AT2G18150 Peroxidase (PER 15) ECM	4.53 (9.92)	5.74	5.15	18.9 (21.86)
AT2G31083 Clavata3	0.06 (0.06)	0.01	0.13	0.02 (0.39)
AT2G33790 Arabinogalactan protein 30	0.26 (0.05)	0	0.08	0 (0.19)
AT2G37440 phosphatidylinositol phosphatase	0.42 (0.31)	0.42	0.59	0.43 (0.24)
AT2G38340 ERF/AP2 TF; DREB subfamily	1.45 (3.73)	4.46	2.23	2.02 (7.54)
AT2G46400 WRKY46	4.26 (2.64)	2.68	4.53	5.75 (2.01)
AT3G28860 MDR1;PGP19	1.11 (1.13)	0.96	0.9	1.22 (1.23)
AT4G15290 similar to cellulose synthase	0.28 (0.42)	0.17	0.1	0.04 (0.29)
AT4G17030 expansin-related (NPA induced)	1.19 (2.32)	2	1.8	2.53 (2.04)
AT4G22950 AGAMOUS-like 19 TF	0.78 (3.74)	3.4	0.35	2.43 (1.44)
AT4G23590 aminotransferase	0.99 (0.43)	0.16	2.01	0.56 (0.37)
AT4G37160 SKS15; pectinesterase-like	0.33 (0.30)	0.06	0.43	0.09 (0.29)
AT5G06720 Peroxidase 53	4.54 (6.00)	4.77	5.03	7.95 (2.44)
AT5G15380 DRM1	4.75 (5.25)	8.45	9.92	7.64 (4.45)
AT5G64060 ANAC103	6.74 (2.39)	5.06	5.83	6.47 (4.66)

**Table 1.** qRT-PCR Assays Confirm Microarray data. qRT-PCR assays of 18 selected genes that, according to microarray data, showed similar up- or down-regulation in dark- and light-grown R2-4A seedlings after the suppression of *APY1* and *APY2*. Changes in the transcript abundance for these genes were assayed at 3.5 and 6.0 d both in dark- and light-grown seedlings. Most gene expression changes persist from 3.5 day to 6 day. Numbers in parentheses are the NimbleGen microarray values for fold-changes, which were only measured in 3.5-d-old dark-grown seedlings and in 6.0-d-old light-grown seedlings. All qRT-PCR numbers represent average fold changes of more than three biological repeats.

TABLE 2a GO terms for Genes upregulated in the light when *APY1* and 2 are suppressed (93)

GO term	Description	Overlap Count	GO count	Adj. P-value
GO:0009627	systemic acquired resistance	9	243	1.32E-06
GO:0050832	defense response to fungus	10	329	1.81E-06
GO:0009862	systemic acquired resistance, salicylic acid mediated	9	266	2.83E-06
GO:0042742	defense response to bacterium	10	362	4.35E-06
GO:0009697	salicylic acid biosynthetic process	8	209	4.66E-06
GO:0010310	regulation of hydrogen peroxide metabolic process	7	185	2.31E-05
GO:0009595	detection of biotic stimulus	5	102	0.000129
GO:0043069	negative regulation of programmed cell death	6	166	0.000133
GO:0000165	MAPK cascade	6	207	0.000456
GO:0010363	regulation of plant-type hypersensitive response	7	368	0.001828
GO:0031348	negative regulation of defense response	6	268	0.001853

Table 2b. GO terms for Genes downregulated in the light when *APY1* and 2 are suppressed (215)

GO term	Description	Overlap Count	GO count	Adj. P-value
GO:0010106	cellular response to iron ion starvation	10	116	2.82E-07
GO:0048765	root hair cell differentiation	10	143	2.06E-06
GO:0006826	iron ion transport	9	117	3.39E-06
GO:0019825	oxygen binding	11	232	2.67E-05
GO:0000041	transition metal ion transport	8	114	2.71E-05
GO:0010054	trichoblast differentiation	5	47	0.000166
GO:0015706	nitrate transport	9	206	0.000347
GO:0010167	response to nitrate	8	195	0.001286
GO:0008194	UDP-glycosyltransferase activity	5	100	0.005826
GO:0016126	sterol biosynthetic process	6	164	0.011485

Table 2c GO terms for Genes upregulated in the dark when *APY1* and 2 are suppressed (333)

GO term	Description	Overlap Count	GO count	Adj. P-value
GO:0006302	double-strand break repair	9	51	9.03E-08
GO:0010332	response to gamma radiation	9	76	3.24E-06
GO:0007275	multicellular organismal development	8	145	0.003286
GO:0010200	response to chitin	15	421	0.00332
GO:0000041	transition metal ion transport	6	114	0.016385
GO:0050832	defense response to fungus	11	329	0.026997
GO:0006355	regulation of transcription, DNA-dependent	31	1412	0.035077
GO:0006261	DNA-dependent DNA replication	5	99	0.036210

Table 2d. GO terms for Genes downregulated in the dark when *APY1* and 2 are suppressed (676)

GO term	Description	Overlap Count	GO count	Adj. P-value
GO:0010106	cellular response to iron ion starvation	18	116	9.67E-09
GO:0010167	response to nitrate	20	195	1.77E-06
GO:0000041	transition metal ion transport	15	114	2.13E-06
GO:0006826	iron ion transport	15	117	3.01E-06
GO:0015706	nitrate transport	20	206	4.35E-06
GO:0055072	iron ion homeostasis	6	26	0.000199
GO:0006865	amino acid transport	10	145	0.032654
GO:0006857	oligopeptide transport	8	105	0.035989

**Table 2.** GO terms with an overlap count of at least 5 that had an adjusted p-value less than 0.05.

In each Table, the number in parentheses is the total number of genes that changed expression.

## REFERENCES

- Almagro, L., Ros, L.V.G., Belchi-Navarro, S., Bru, R., Barcelo, A.R., and Pedreno, M.A.** (2009). Class III peroxidases in plant defence reactions. *Journal of Experimental Botany* 60:377-390.
- Aquea, F., Federici, F., Moscoso, C., Vega, A., Julian, P., Haseloff, J., and Arce-Johnson, P.** (2012). A molecular framework for the inhibition of *Arabidopsis* root growth in response to boron toxicity. *Plant Cell and Environment* 35:719-734.
- Chiu, T.Y., Christiansen, K., Moreno, I., Lao, J.M., Loque, D., Orellana, A., Heazlewood, J.L., Clark, G., and Roux, S.J.** (2012). AtAPY1 and AtAPY2 Function as Golgi-Localized Nucleoside Diphosphatases in *Arabidopsis thaliana*. *Plant and Cell Physiology* 53:1913-1925.
- Chivasa, S., Murphy, A.M., Hamilton, J.M., Lindsey, K., Carr, J.P., and Slabas, A.R.** (2009). Extracellular ATP is a regulator of pathogen defence in plants. *Plant Journal* 60:436-448.
- Clark, G., and Roux, S.J.** (2009). Extracellular nucleotides: Ancient signaling molecules. *Plant Science* 177.
- Clark, G., and Roux, S.J.** (2011). Apyrases, extracellular ATP and the regulation of growth. *Current Opinion in Plant Biology* 14:700-706.
- Clark, G., Torres, J., Finlayson, S., Guan, X.Y., Handley, C., Lee, J., Kays, J.E., Chen, Z.J., and Roux, S.J.** (2010a). Apyrase (Nucleoside Triphosphate-Diphosphohydrolase) and Extracellular Nucleotides Regulate Cotton Fiber Elongation in Cultured Ovules. *Plant Physiology* 152:1073-1083.
- Clark, G., Wu, M., Wat, N., Onyirimba, J., Pham, T., Herz, N., Ogoti, J., Gomez, D., Canales, A.A., Aranda, G., et al.** (2010b). Both the stimulation and inhibition of root hair growth induced by extracellular nucleotides in *Arabidopsis* are mediated by nitric oxide and reactive oxygen species. *Plant Molecular Biology* 74:423-435.
- Demidchik, V., Nichols, C., Oliynyk, M., Dark, A., Glover, B.J., and Davies, J.M.** (2003). Is ATP a signaling agent in plants? *Plant Physiology* 133.
- Demidchik, V., Shang, Z., Shin, R., Colaco, R., Laohavosit, A., Shabala, S., and Davies, J.M.** (2011). Receptor-Like Activity Evoked by Extracellular ADP in *Arabidopsis* Root Epidermal Plasma Membrane. *Plant Physiology* 156:1375-1385.
- Demidchik, V., Shang, Z., Shin, R., Thompson, E., Rubio, L., Laohavosit, A., Mortimer, J.C., Chivasa, S., Slabas, A.R., Glover, B.J., et al.** (2009). Plant extracellular ATP signalling by plasma membrane NADPH oxidase and Ca<sup>2+</sup> channels. *Plant Journal* 58:903-913.
- Djebali, N., Mhadhbi, H., Lafitte, C., Dumas, B., Esquerre-Tugaye, M.T., Aouani, M.E., and Jacquet, C.** (2011). Hydrogen peroxide scavenging mechanisms are components of *Medicago truncatula* partial resistance to *Aphanomyces euteiches*. *European Journal of Plant Pathology* 131:559-571.
- Dufrene, Y.F., van der Wal, A., Norde, W., and Rouxhet, P.G.** (1997). X-ray photoelectron spectroscopy analysis of whole cells and isolated cell walls of gram-positive bacteria: comparison with biochemical analysis. *Journal of bacteriology* 179:1023-1028.
- Dunand, C., Crevecoeur, M., and Penel, C.** (2007). Distribution of superoxide and hydrogen peroxide in *Arabidopsis* root and their influence on root development: possible interaction with peroxidases. *New Phytologist* 174:332-341.

- Fleischer, A., Titel, C., and Ehwald, R.** (1998). The Boron Requirement and Cell Wall Properties of Growing and Stationary Suspension-Cultured *Chenopodium album* L. Cells. *Plant Physiol.* 117:1401-1410.
- Franza, T., and Expert, D.** (2013). Role of iron homeostasis in the virulence of phytopathogenic bacteria: an "a la carte' menu. *Molecular Plant Pathology* 14:429-438.
- Gapper, C., and Dolan, L.** (2006). Control of plant development by reactive oxygen species. *Plant Physiology* 141:341-345.
- Gazarian, I.G., Lagrimini, L.M., Mellon, F.A., Naldrett, M.J., Ashby, G.A., and Thorneley, R.N.F.** (1998). Identification of skatolyl hydroperoxide and its role in the peroxidase-catalysed oxidation of indol-3-yl acetic acid. *Biochemical Journal* 333:223-232.
- Go, Y.S., Lee, S.B., Kim, H.J., Kim, J., Park, H.Y., Kim, J.K., Shibata, K., Yokota, T., Ohyama, K., Muranaka, T., et al.** (2012). Identification of marneral synthase, which is critical for growth and development in *Arabidopsis*. *Plant Journal* 72:791-804.
- Hosmani, P.S., Kamiya, T., Danku, J., Naseer, S., Geldner, N., Guerinot, M.L., and Salt, D.E.** (2013). Dirigent domain-containing protein is part of the machinery required for formation of the lignin-based Caspary strip in the root. *Proceedings of the National Academy of Sciences of the United States of America* 110:14498-14503.
- Ishii, T., Matsunaga, T., Pellerin, P., O'Neill, M.A., Darvill, A., and Albersheim, P.** (1999). The Plant Cell Wall Polysaccharide Rhamnogalacturonan II Self-assembles into a Covalently Cross-linked Dimer. *The Journal of biological chemistry* 274:13098-13104.
- Jeter, C.R., Tang, W.Q., Henaff, E., Butterfield, T., and Roux, S.J.** (2004). Evidence of a novel cell signaling role for extracellular adenosine triphosphates and diphosphates in *Arabidopsis*. *Plant Cell* 16:2652-2664.
- Jolie, R.P., Duvetter, T., Van Loey, A.M., and Hendrickx, M.E.** (2010). Pectin methylesterase and its proteinaceous inhibitor: a review. *Carbohydr. Res.* 345:2583-2595.
- Kempel, A., Schadler, M., Chrobock, T., Fischer, M., and van Kleunen, M.** (2011). Tradeoffs associated with constitutive and induced plant resistance against herbivory. *Proceedings of the National Academy of Sciences of the United States of America* 108:5685-5689.
- Kim, S.-Y., Sivaguru, M., and Stacey, G.** (2006). Extracellular ATP in plants. Visualization, localization, and analysis of physiological significance in growth and signaling. *Plant Physiology* 142.
- Knowles, A.F.** (2011). The GDA1\_CD39 superfamily: NTPDases with diverse functions. *Purinergic Signalling* 7:21-45.
- Kobayashi, T., and Nishizawa, N.K.** (2012). Iron Uptake, Translocation, and Regulation in Higher Plants. *Annual Review of Plant Biology*, Vol 63 63:131-152.
- Krylov, S.N., and Dunford, H.B.** (1996). Detailed model of the peroxidase-catalyzed oxidation of indole-3-acetic acid at neutral pH. *Journal of Physical Chemistry* 100:913-920.
- Liu, X., Wu, J., Clark, G., Lundy, S., Lim, M., Arnold, D., Chan, J., Tang, W., Muday, G., Gardner, G., et al.** (2012). Role for apyrases in polar auxin transport in *Arabidopsis*. *Plant Physiology* 160:1985-1995.
- Lloyd, A.J., William Allwood, J., Winder, C.L., Dunn, W.B., Heald, J.K., Cristescu, S.M., Sivakumaran, A., Harren, F.J., Mulema, J., Denby, K., et al.** (2011). Metabolomic approaches reveal that cell wall modifications play a major role in ethylene-mediated resistance against *Botrytis cinerea*. *Plant J.* 67:852-868.

- Markakis, M.N., De Cnodder, T., Lewandowski, M., Simon, D., Boron, A., Balcerowicz, D., Doubbo, T., Taconnat, L., Renou, J.P., Hofte, H., et al.** (2012). Identification of genes involved in the ACC-mediated control of root cell elongation in *Arabidopsis thaliana*. *Bmc Plant Biology* 12.
- Mouille, G., Robin, S., Lecomte, M., Pagant, S., and Höfte, H.** (2003). Classification and identification of *Arabidopsis* cell wall mutants using Fourier-Transform InfraRed (FT-IR) microspectroscopy. *Plant J.* 35:393-404.
- Moulder, J.F., Stickle, W.F., Sobol, P.E., and Bomben, K.D.** (1992). *Handbook of X-ray Photoelectron Spectroscopy*: Physical Electronics, Inc.
- Nakagami, H., Soukupova, H., Schikora, A., Zarsky, V., and Hirt, H.** (2006). A mitogen-activated protein kinase kinase kinase mediates reactive oxygen species homeostasis in *Arabidopsis*. *Journal of Biological Chemistry* 281:38697-38704.
- Naseer, S., Lee, Y., Lapierre, C., Franke, R., Nawrath, C., and Geldner, N.** (2012). Caspary strip diffusion barrier in *Arabidopsis* is made of a lignin polymer without suberin. *Proceedings of the National Academy of Sciences of the United States of America* 109:10101-10106.
- Nemhauser, J.L., Hong, F.X., and Chory, J.** (2006). Different plant hormones regulate similar processes through largely nonoverlapping transcriptional responses. *Cell* 126:467-475.
- Nivens, D.E., Ohman, D.E., Williams, J., and Franklin, M.J.** (2001). Role of Alginate and Its O Acetylation in Formation of *Pseudomonas aeruginosa* Microcolonies and Biofilms. *J. Bacteriol.* 183:1047-1057.
- O'Neill, M.A., Ishii, T., Albersheim, P., and Darvill, A.G.** (2004). Rhamnogalacturonan II: Structure and Function of a Borate Cross-Linked Cell Wall Pectic Polysaccharide. *Annu. Rev. Plant Biol.* 55:109-139.
- Palin, R., and Geitmann, A.** (2012). The role of pectin in plant morphogenesis. *Biosystems* 109:397-402.
- Passardi, F., Cosio, C., Penel, C., and Dunand, C.** (2005). Peroxidases have more functions than a Swiss army knife. *Plant Cell Reports* 24:255-265.
- Passardi, F., Penel, C., and Dunand, C.** (2004). Performing the paradoxical: how plant peroxidases modify the cell wall. *Trends in Plant Science* 9:534-540.
- Pau-Roblot, C., Petit, E., Sarazin, C., Courtois, J., Courtois, B., Barbotin, J.N., and Séguin, J.P.** (2002). Studies of low molecular weight samples of glucuronans with various acetylation degree. *Biopolymers* 64:34-43.
- Pedreira, J., Herrera, M.T., Zarra, I., and Revilla, G.** (2011). The overexpression of AtPrx37, an apoplastic peroxidase, reduces growth in *Arabidopsis*. *Physiologia Plantarum* 141:177-187.
- Peer, W.A., Blakeslee, J.J., Yang, H.B., and Murphy, A.S.** (2011). Seven Things We Think We Know about Auxin Transport. *Molecular Plant* 4:487-504.
- Potters, G., Pasternak, T.P., Guisez, Y., and Jansen, M.A.K.** (2009). Different stresses, similar morphogenic responses: integrating a plethora of pathways. *Plant Cell and Environment* 32:158-169.
- Potters, G., Pasternak, T.P., Guisez, Y., Palme, K.J., and Jansen, M.A.K.** (2007). Stress-induced morphogenic responses: growing out of trouble? *Trends in Plant Science* 12:98-105.

- Ramstedt, M., Nakao, R., Wai, S.N., Uhlin, B.E., and Boily, J.-F.** (2011). Monitoring surface chemical changes in the bacterial cell wall: multivariate analysis of cryo-x-ray photoelectron spectroscopy data. *The Journal of biological chemistry* 286:12389-12396.
- Reichler, S.A., Torres, J., Rivera, A.L., Cintolesi, V.A., Clark, G., and Roux, S.J.** (2009). Intersection of two signalling pathways: extracellular nucleotides regulate pollen germination and pollen tube growth via nitric oxide. *Journal of Experimental Botany* 60.
- Reid, R.J., Hayes, J.E., Post, A., Stangoulis, J.C.R., and Graham, R.D.** (2004). A critical analysis of the causes of boron toxicity in plants. *Plant Cell and Environment* 27:1405-1414.
- Ridley, B.L., O'Neill, M.A., and Mohnen, D.** (2001). Pectins: structure, biosynthesis, and oligogalacturonide-related signaling. *Phytochemistry* 57:929-967.
- Roux, S.J., and Steinebrunner, I.** (2007). Extracellular ATP: an unexpected role as a signaler in plants. *Trends in Plant Science* 12:522-527.
- Salmi, M., Clark, G., and Roux, S.** (2013). Current status and proposed roles for nitric oxide as a key mediator of the effects of extracellular nucleotides on plant growth. *Frontiers in Plant Science* 4:1-7.
- Sampedro, J., and Cosgrove, D.J.** (2005). The expansin superfamily. *Genome Biology* 6.
- Sasidharan, R., Voesenek, L., and Pierik, R.** (2011). Cell Wall Modifying Proteins Mediate Plant Acclimatization to Biotic and Abiotic Stresses. *Critical Reviews in Plant Sciences* 30:548-562.
- Schiller, M., Massalski, C., Kurth, T., and Steinebrunner, I.** (2012). The Arabidopsis apyrase AtAPY1 is localized in the Golgi instead of the extracellular space. *Bmc Plant Biology* 12.
- Song, C.J., Steinebrunner, I., Wang, X.Z., Stout, S.C., and Roux, S.J.** (2006). Extracellular ATP induces the accumulation of superoxide via NADPH oxidases in Arabidopsis. *Plant Physiology* 140:1222-1232.
- Steinebrunner, I., Wu, J., Sun, Y., Corbett, A., and Roux, S.J.** (2003). Disruption of apyrases inhibits pollen germination in arabidopsis. *Plant Physiology* 131.
- Suzuki, H., Dowd, P.F., Johnson, E.T., Hum-Musser, S.M., and Musser, R.O.** (2012). Effects of Elevated Peroxidase Levels and Corn Earworm Feeding on Gene Expression in Tomato. *Journal of Chemical Ecology* 38:1247-1263.
- Tanaka, K., Gilroy, S., Jones, A.M., and Stacey, G.** (2010a). Extracellular ATP signaling in plants. *Trends in Cell Biology* 20:601-608.
- Tanaka, K., Swanson, S.J., Gilroy, S., and Stacey, G.** (2010b). Extracellular Nucleotides Elicit Cytosolic Free Calcium Oscillations in Arabidopsis. *Plant Physiology* 154:705-719.
- Tang, W.Q., Brady, S.R., Sun, Y., Muday, G.K., and Roux, S.J.** (2003). Extracellular ATP inhibits root gravitropism at concentrations that inhibit polar auxin transport. *Plant Physiology* 131:147-154.
- Torres, J., Rivera, A., Clark, G., and Roux, S.J.** (2008). PARTICIPATION OF EXTRACELLULAR NUCLEOTIDES IN THE WOUND RESPONSE OF DASYCLADUS VERMICULARIS AND ACETABULARIA ACETABULUM (DASYCLADES, CHLOROPHYTA). *Journal of Phycology* 44.
- Tsang, D.L., Edmond, C., Harrington, J.L., and Nuhse, T.S.** (2011). Cell Wall Integrity Controls Root Elongation via a General 1-Aminocyclopropane-1-Carboxylic Acid-Dependent, Ethylene-Independent Pathway. *Plant Physiology* 156:596-604.

- Tsukagoshi, H.** (2012). Defective root growth triggered by oxidative stress is controlled through the expression of cell cycle-related genes. *Plant Science* 197:30-39.
- Tsukagoshi, H., Busch, W., and Benfey, P.N.** (2010). Transcriptional Regulation of ROS Controls Transition from Proliferation to Differentiation in the Root. *Cell* 143:606-616.
- Tusher, V.G., Tibshirani, R., and Chu, G.** (2001). Significance analysis of microarrays applied to the ionizing radiation response. *Proceedings of the National Academy of Sciences of the United States of America* 98:5116-5121.
- Vincken, J.P., Schols, H.A., Oomen, R., McCann, M.C., Ulvskov, P., Voragen, A., and Visser, R.** (2003). If Homogalacturonan Were a Side Chain of Rhamnogalacturonan I. Implications for Cell Wall Architecture. *Plant Physiol.* 132:1781-1789.
- Walters, D., and Heil, M.** (2007). Costs and trade-offs associated with induced resistance. *Physiological and Molecular Plant Pathology* 71:3-17.
- Wolf, S., Hematy, K., and Hofte, H.** (2012). Growth Control and Cell Wall Signaling in Plants. *Annual Review of Plant Biology*, Vol 63 63:381-407.
- Wu, J., Steinebrunner, I., Sun, Y., Butterfield, T., Torres, J., Arnold, D., Gonzalez, A., Jacob, F., Reichler, S., and Roux, S.J.** (2007). Apyrases (nucleoside triphosphate-diphosphohydrolases) play a key role in growth control in arabidopsis. *Plant Physiology* 144:961-975.
- Wu, S.J., Liu, Y.S., and Wu, J.Y.** (2008). The signaling role of extracellular ATP and its dependence on Ca(2) flux in elicitation of *Salvia miltiorrhiza* hairy root cultures. *Plant and Cell Physiology* 49:617-624.
- Zhang, K.W., Bhuiya, M.W., Pazo, J.R., Miao, Y.C., Kim, H., Ralph, J., and Liu, C.J.** (2012). An Engineered Monolignol 4-O-Methyltransferase Depresses Lignin Biosynthesis and Confers Novel Metabolic Capability in Arabidopsis. *Plant Cell* 24:3135-3152.

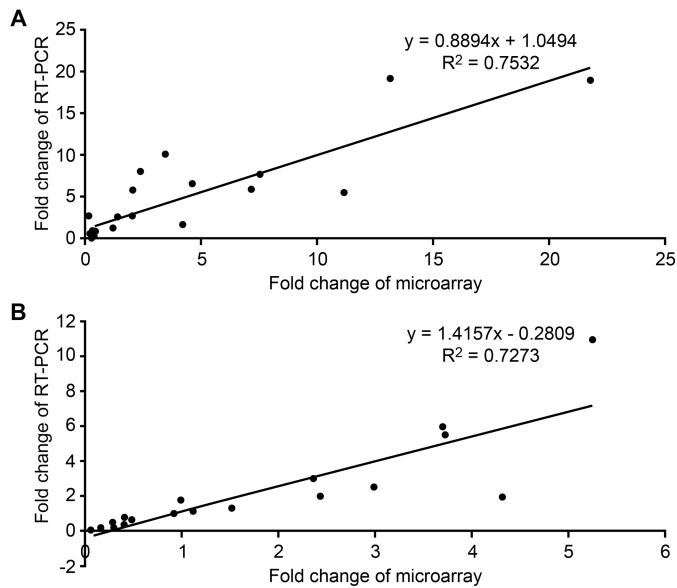


**Figure 1.** Correlation Analyses between Real-Time qRT-PCR and Microarray Results. Quantitative real-time qRT-PCR was used to validate the two microarray data sets. (A) Result of standard linear regression analysis between the fold changes observed in apyrase-suppressed light-grown plants by real-time qRT-PCR (X axis) and microarray analyses (Y axis). (B) Result of standard linear regression analysis between the fold changes observed in apyrase-suppressed dark-grown plants by real-time qRT-PCR (X axis) and microarray data (Y axis). The calculated equation and correlation value ( $R^2$ ) are shown along with the regression line.

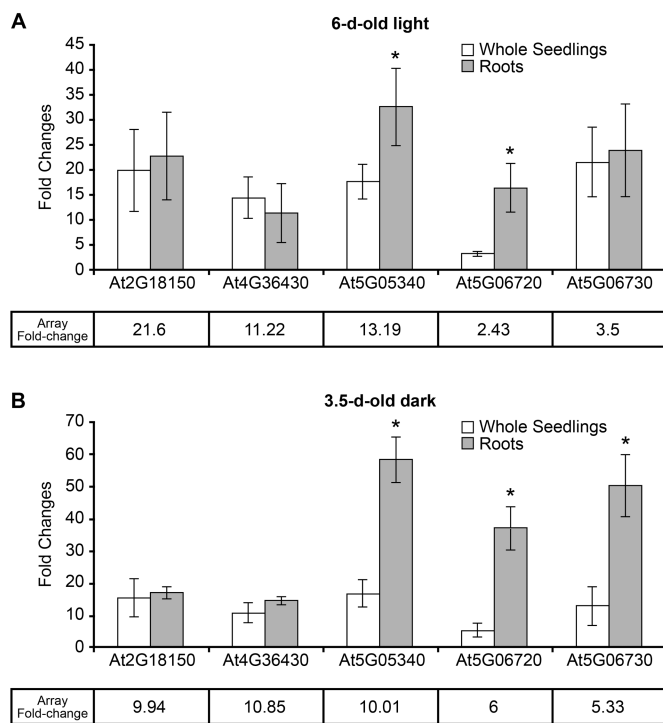


**Figure 2.** Transcript Abundance of Five Genes Encoding Type III Wall Peroxidases in Whole Seedlings and Roots Increases in R2-4A Mutants Suppressed in Their Expression of *APY1* and *APY2*. (A) qRT-PCR results of the transcript abundance changes of 5 peroxidase genes in light-grown 6-d-old seedlings. (B) qRT-PCR results of the transcript abundance changes of 5 peroxidase genes in dark-grown 3.5-d-old seedlings. Fold changes for each gene in microarray analysis is also presented in each graph. Error bars represent standard deviation. At least three biological repeats were performed for this experiment.

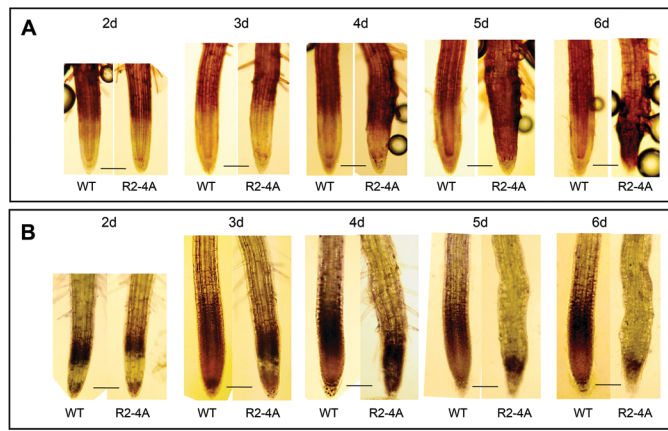


**Figure 3.** Higher ROS levels Are Induced R2-4A Roots When *APY1* and *APY2* Are Suppressed. (A) Hydrogen peroxide levels in wild-type (WT) and R2-4A roots from 2 d to 6 d after estradiol treatment. DAB (3, 3'-diaminobenzidine tetrahydrochloride) was used to stain hydrogen peroxide. (B) Superoxide levels in WT and R2-4A roots from 2 d to 6 d. NBT (nitroblue tetrazolium) was used to stain superoxide. Images are representative of at least three biological repeats. Scale bar = 100  $\mu$ m.

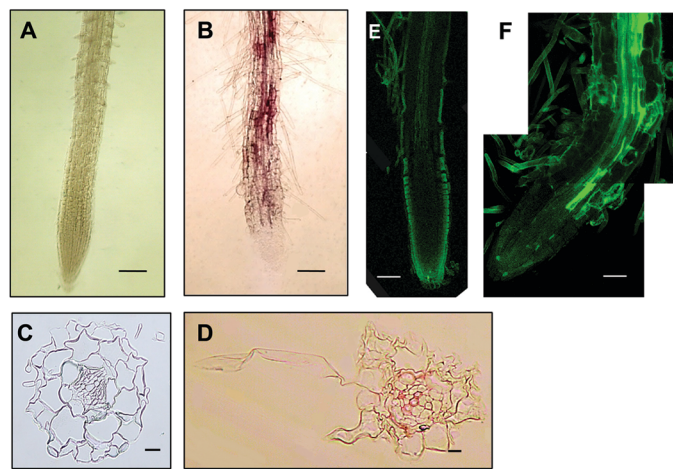


**Figure 4.** Higher Lignin Levels Are Induced in R2-4A Roots When *APY1* and *APY2* Are Suppressed. Lignin staining of 6-d-old roots with phloroglucinol in (A) wild-type (WT) and (B) R2-4A roots. Magenta color indicates lignin. Cross sections of (C) WT and (D) R2-4A roots stained with phloroglucinol. Cross sections are from region 200~600  $\mu\text{m}$  from root tip where vascular tissue is not fully matured in WT. Lignin auto-fluorescence of WT (E) and R2-4A (F). Images are representative of at least three biological repeats. Scale bar = 100  $\mu\text{m}$  in (A) and (B), 10  $\mu\text{m}$  in (C) and (D), and 50  $\mu\text{m}$  in (E) and (F).

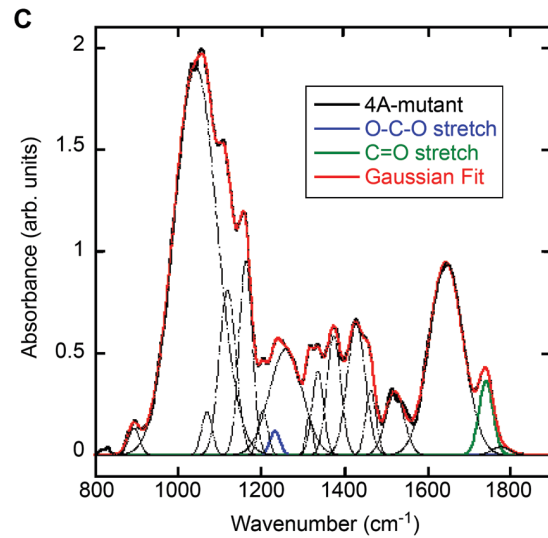
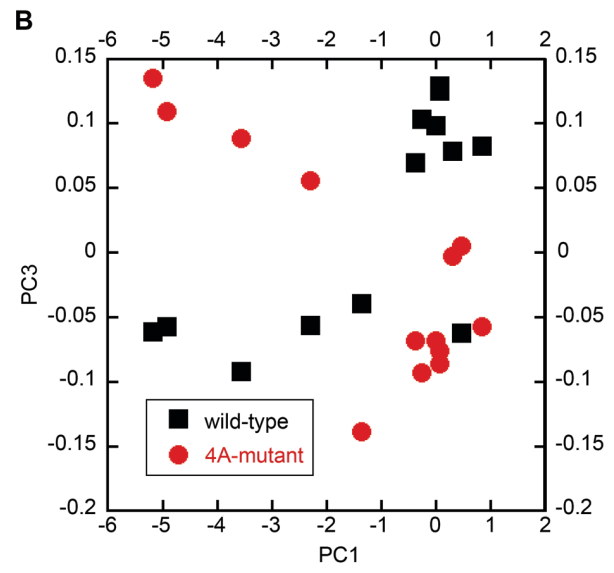
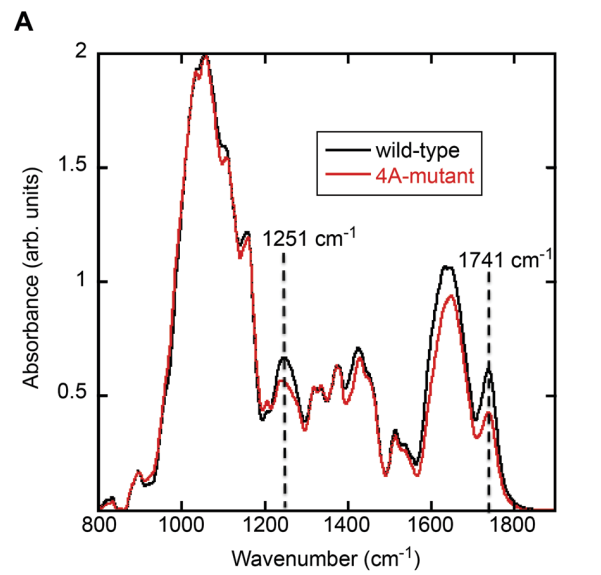


**Figure 5.** Cell Walls of *Arabidopsis* Isolated from R2-4A Mutants Suppressed in Their Expression of *APY1* and *APY2* Have Altered FTIR Spectra Indicating Fewer Methyl Ester Linkages. (A) Averaged FTIR spectra for wild-type (black) and R2-4A mutant (red) samples. The average signal was computed using 13 spectra for the mutant and 13 for the wild-type samples. Each of the spectra were obtained from 100 scans at a resolution of  $4\text{ cm}^{-1}$ . The averaged spectra were normalized to the maximum intensity peak at  $1056\text{ cm}^{-1}$  peak then baseline corrected. Dashed lines are added to highlight differences in the two spectra at  $1251$  and  $1741\text{ cm}^{-1}$ . (B) Principal component analysis (PCA) of wild-type (black squares) and mutant (red circles) samples. PC1 is plotted against PC3, accounting for 99.3% of the variance. Each point on the figure represents one of the 13 peaks selected for analysis ( $1035, 1057, 1111, 1161, 1207, 1251, 1319, 1336, 1374, 1431, 1516, 1648$ , and  $1741\text{ cm}^{-1}$ ). (C) An average spectrum of the 4A mutant samples (black) is shown here with 17 fitted Gaussian curves along with the total Gaussian fit (red). The Gaussian fits associated with stretches arising from methyl-ester groups are highlighted in green, ( $1742\text{ cm}^{-1}$ ) and blue ( $1234\text{ cm}^{-1}$ ), which correspond to C=O and O-C-O vibrations, respectively.

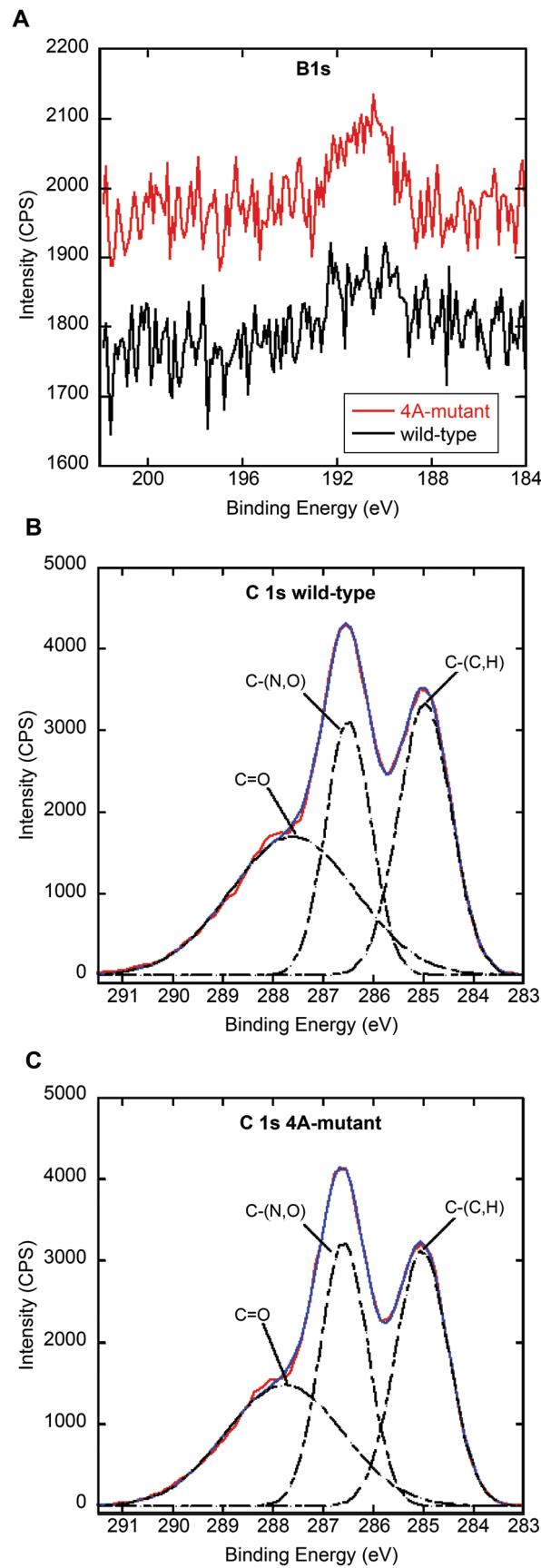


**Figure 6.** Cell Walls of *Arabidopsis* Isolated from R2-4A Mutants Suppressed in Their Expression of *APY1* and *APY2* Have Altered XP Spectra Indicating More Boron Linkages. (A) XP spectra of the B 1s region showing a peak near 190 eV for wild-type (black) and mutant (red) samples. Scans were taken at a resolution of 0.1 eV, 300 ms dwell time, and a detector aperture of 160 mm. The carbon 1s region of XP spectra of (B) wild-type and (C) R2-4A-mutant cell walls taken at a resolution of 0.1 eV, dwell time of 3000 ms, and a detector aperture of 20 mm. Spectral decomposition was done by fitting the peaks to Gaussian curves. The baseline corrected data is shown in red, Gaussian fit in blue, and peak composites as dashed lines. The aliphatic carbon (C-(C,H)) peak was adjusted to 285 eV to account for binding energy shifts due to the use of a charge neutralizer. Peaks at 286.6 and 287.8 eV correspond to C-(N,O) and C=O functional groups, respectively. When measured with respect to the 285 eV signal, the R2-4A mutant sample shows a 20% increase in the 286.6 eV peak over the wild-type.

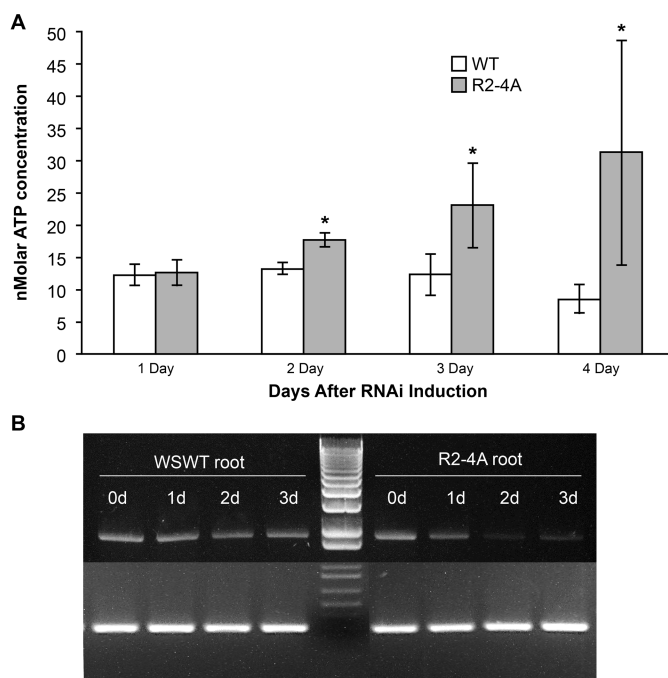


**Figure 7.** Media [eATP] Rises with Increased Suppression of Apyrase Expression in R2-4A Seedlings. (A) Time course of increase of [ATP] in seedling growth media, based on luciferase assay luminescence in comparison to ATP standard curve. Error bars represent standard deviation, and asterisks indicate statistical significance based on p value >0.05 in a Student's t-test (B) Time course of loss of *APY1* transcripts during continuous treatment of R2-4A mutants with estradiol inducer of RNAi construct.